6-13-2023

Nonlinear impact-echo test for quantitative evaluation of ASR damage in concrete

Clayton Malone

Hongbin Sun

Jinying Zhu

Nonlinear impact-echo test for quantitative evaluation of ASR damage in concrete

Clayton Malone
University of Nebraska–Lincoln
Hongbin Sun
Oak Ridge National Laboratory
Jinying Zhu (jyzhu@unl.edu)
University of Nebraska–Lincoln

Research Article

Keywords: Nonlinear, acoustics, Impact-echo, Alkali-Silica Reaction, Concrete 1

Posted Date: June 13th, 2023

DOI: https://doi.org/10.21203/rs.3.rs-3039855/v1

Additional Declarations: Competing interest reported. The corresponding author Jinying Zhu serves on the editorial board of Journal of Nondestructive Evaluation.

Version of Record: A version of this preprint was published at Journal of Nondestructive Evaluation on October 28th, 2023. See the published version at https://doi.org/10.1007/s10921-023-01003-2.

Published (2023) Journal of Nondestructive Evaluation, 42 (4), art. no. 93, .DOI: 10.1007/s10921-023-01003-2

Nonlinear impact-echo test for quantitative evaluation of ASR damage in concrete

Clayton Malone[1], Hongbin Sun[2], Jinying Zhu[1*]

[1*]Department of Civil and Environmental Engineering, University of Nebraska Lincoln, 1110 S 67TH ST, Omaha, 68118, NE, USA.
[2]Oak Ridge National Laboratory, P.O. Box 2008, Oak Ridge, 37831, TN, USA.

*Corresponding author(s). E-mail(s): jyzhu@unl.edu;
Contributing authors: cmalone@huskers.unl.edu; sunh1@ornl.gov;

Abstract

Nonlinear acoustic methods demonstrate high sensitivity for concrete damage evaluation. Among these methods, nonlinear resonance acoustic methods have been widely used in laboratory tests on small scale test samples. In this study, a nonlinear impact-echo (IE) method was proposed for concrete damage evaluation, in which the IE frequency shift was measured at different impact force levels. The nonlinear IE test is similar to the nonlinear impact resonance acoustic spectroscopy (NIRAS) test in the experimental setup and analysis method. However, the nonlinear IE test excites a local thickness resonance mode of a member instead of the global resonance vibration. Therefore, the analyzed mode is not affected by boundary conditions and can be applied to large concrete structural members. To identify the fundamental IE frequency, multiple impacts at different locations were used. The nonlinear IE method was then validated on seven concrete beam specimens with different levels of alkali-silica reaction (ASR) damage. The nonlinear IE test results demonstrate high sensitivity to concrete damage and allow for quantitative assessment of the damage state of concrete without a baseline measurement.

Keywords: Nonlinear, acoustics, Impact-echo, Alkali-Silica Reaction, Concrete

1 Introduction

Nonlinear acoustic techniques have gained attention in the nondestructive testing (NDT) field because of their high sensitivity to microcracking damage when compared to linear acoustic methods. In materials with complex microstructures, such as concrete, microcracks smaller than the aggregates might not cause significant change of linear acoustic parameters (wave velocity, resonance frequencies), but they will induce high acoustic nonlinearity. Nonlinear acoustic responses may include material softening with strain, high harmonics, or side band frequencies. Softening is shown as a decrease of the Young's modulus with increasing strain, which can be measured by monitoring the change in resonance frequency or wave velocity under different strain levels.

A common nonlinear acoustic test in laboratory testing is the nonlinear resonance acoustic spectroscopy (NRAS) method [1]. NRAS measures the resonance frequency shift Δf when a sample is excited by frequency sweeps around the resonance frequency at different strain levels. Chen et al. [2] proposed using an impact hammer to induce the flexural mode resonance of a sample and measure the resonance frequency shift under different impact amplitudes. This method is called "Nonlinear Impact Resonance Acoustic Spectroscopy" (NIRAS), which can be regarded as a nonlinear version of the resonant frequency test in accordance with ASTM C215 [3]. The impact method is simple in test setup and analysis. In both NRAS and NIRAS methods, the strain levels are very low, so an accelerometer is typically used to measure the resonant response (acceleration). The relationship between the relative frequency shift and the acceleration amplitude is defined as the nonlinear parameter. Dynamic acoustoelastic testing (DAET) measures ultrasonic wave velocity change due to dynamic modulation by a low frequency (LF) acoustic wave [4–6]. Nonlinear parameters are extracted from the correlation curves between the relative velocity change of ultrasonic pulses and the instantaneous LF amplitude (or strain). The DAET method provides more details

about hysteresis, transient elastic softening, and slow relaxation than the vibration based methods.

Although these nonlinear ultrasonic testing methods show different degrees of success in laboratory tests, there are several major limitations that hinder application of these methods in practice. First, these tests are only applicable to small samples. The NRAS test needs to excite the free vibration of the tested sample, and DAET uses a shake table or large piezoelectric disk to vibrate the sample to generate strain changes inside the sample. These methods are difficult to apply to large concrete structures. Second, because global free vibration modes are excited, the resonance frequency and nonlinear response not only depend on material properties and specimen dimensions, but also depend on boundary and support conditions. These tests cannot be simply extended to concrete structural members because of various types of end supports in real structures. Some recent studies have applied nonlinear ultrasonic tests to large-scale concrete specimens and structures with promising results [7, 8], but these methods either need high power input sources or the results are qualitative for damage evaluation.

The impact-echo (IE) test is a widely used NDT method for evaluation of various types of concrete structures [9], including plates and columns. Since the IE test only needs to access one side of a concrete member and the frequency only depends on the thickness of a plate, and aspect ratio of cross-sections for beams and columns, it can be applied to large concrete structures such as plates, beams, and columns. When the IE test is used for evaluation of concrete deterioration, the change of the frequency or wave velocity is investigated. However, these parameters alone are not sufficient for quantitative assessment of concrete deterioration with microcracking unless baseline measurements on reference samples are available.

In this paper, a nonlinear IE method is proposed for concrete damage evaluation. Similar to the NIRAS test, which measures the resonance mode of small concrete

samples, the fundamental IE mode of concrete specimens is measured under multiple impacts with increasing amplitudes. The relative IE frequency shift is correlated with the amplitude of the impact responses, and a nonlinear parameter (α) is extracted from the correlation. A control concrete specimen and specimens with different levels of alkali-silica reaction (ASR) damage were studied using the nonlinear IE method.

2 Theoretical background of resonance modes in bars

2.1 Linear impact-echo theory

In a plate, the IE test measures a local resonance mode with a frequency related to the member thickness h and the P wave velocity V_P as $f = \beta_{IE} V_P / 2h$. Gibson and Popovics [10] proved that the local resonance mode is a non-propagating Lamb wave S_1 mode at the zero-group-velocity (S_1ZGV), and the parameter β_{IE} only depends on Poisson's ratio. Higher order ZGV modes may also be detectable in a plate, such as the A_2ZGV mode, but the S_1ZGV mode dominates in most cases. Prada et al. [11] presented an extensive study on the existence of ZGV modes and their frequencies for different Poisson's ratios.

The IE test has also been applied to beams and columns [12]. Similar to plates, these modes also correspond to ZGV modes or cutoff frequency modes (zero wave number) [13]. The ZGV frequencies can be obtained from dispersion curves by solving the dispersion equation for cylindrical structures. Dispersion curves for a bar with a non-cylindrical cross-section should be solved using a semi-analytical finite element method [14]. Unlike in plates, there are many ZGV and cut-off frequencies in a rod within a narrow frequency range. Therefore, a hammer impact on a beam or column often excites multiple modes. The fundamental mode is typically analyzed. For beams and columns, the IE frequencies can still be expressed in the form of $f = \beta_{IE} V_P / 2D$

[12] where D is the thickness in the test direction, and β_{IE} depends on the cross-section geometry of the specimen (circle, square, or rectangle) and Poisson's ratio. For a concrete member with a square cross-section, Lin and Sansalone found that β_{IE} is around 0.87 [15] for the fundamental IE mode, which increases slightly with a smaller Poisson's ratio.

2.2 Nonlinear acoustic theory

Concrete is a nonlinear material with complex mesoscopic structures. The nonlinearity of concrete comes from the mesoscopic linkages (order 10^{-6} to 10^{-9} m) among the cement, aggregates, and cracks. Cracks and microcracks in concrete will dramatically increase the concrete material nonlinearity. The presence of nonlinearity in concrete is observed in the hysteresis found in its stress-strain relationship and its discrete memory [16]. A nonlinear hysteresis model describes the strain and strain rate related modulus as [17]:

$$E(\varepsilon, \dot{\varepsilon}) = E_0 \left\{1 - \beta\varepsilon - \delta\varepsilon^2 - \alpha\left[\Delta\varepsilon + \varepsilon \text{sign}(\dot{\varepsilon})\right]\right\} \tag{1}$$

where E_0 is the linear modulus, ε and $\dot{\varepsilon}$ are the strain and strain rate, respectively, β and δ are the quadratic and cubic nonlinear parameters, and α represents the hysteresis parameter. The function $\text{sign}(\dot{\varepsilon}) = 1$ if $\dot{\varepsilon} > 0$ and $\text{sign}(\dot{\varepsilon}) = -1$ if $\dot{\varepsilon} < 0$.

Nonlinear acoustic techniques demonstrate higher sensitivity to micro-damage when compared to linear acoustic methods. Many nonlinear acoustic methods are based on the principle that the elastic modulus will decrease (softening) with increasing strain, as described in Eq. 1. Nonlinear acoustic methods usually generate larger strain (10^{-6} to 10^{-5}) on materials than linear methods (10^{-7}). The nonlinearity is determined from the strain-induced changes in acoustic properties, such as frequency shift and velocity changes [18]. For example, in the NRAS method, the relative resonance

frequency shift is related to the strain change as [1]:

$$\frac{f_0 - f}{f_0} = \alpha_\varepsilon \Delta\varepsilon = \alpha_a \Delta a \tag{2}$$

where α_ε is proportional to the absolute nonlinear parameter α in Eq. 1, Δa is the acceleration amplitude, f_0 is the linear resonant frequency measured at a low strain level, and f is the frequency at a high strain level. In most experiments, the relative nonlinear parameter α_a is used because the vibration acceleration a is easier to measure than the strain ε.

2.3 Nonlinear impact-echo

Unlike global vibration modes, the local resonance modes measured in the IE test are not affected by boundary conditions. Therefore, the IE test is applicable to large size concrete plates, beams, and columns. By extending the nonlinear resonance theory in Eq. 2 and NIRAS test method to the IE test, a nonlinear acoustic test can be performed on large concrete specimens. When multiple impacts are applied to the specimen, the IE frequency will decrease with increasing impact amplitudes. Like in the NIRAS test, the strain in Eq. 1 can be replaced by dynamic response parameters such as velocity or acceleration, because the maximum strain is linearly related to the maximum velocity and acceleration [19].

3 Finite element simulations

Finite element simulations were conducted using Abaqus® to confirm the fundamental IE modes tested in this study. Modal analyses were performed on 2D (0.30 m × 0.30 m) and 3D concrete models (0.30 m × 0.30 m × 1.10 m) with a mesh size of 8 mm. The material properties used in the simulation were as follows: density ρ = 2410 kg/m^3, Young's modulus E = 40,000 MPa, and Poisson's ratio ν = 0.15. These

parameters give a P-wave velocity (V_p) of approximately 4200 m/s, which agrees with the experimental values measured on concrete specimens.

Figure 1 shows the fundamental IE modes using the 2D (plane strain) and 3D models, which give the IE frequencies of 6319 Hz and 6266 Hz, respectively. The frequency of the 2D model represents the cutoff frequency (zero wave number), while the frequency from the 3D model represents a local ZGV mode. The β_{IE} parameter is calculated as 0.89 for the given material properties.

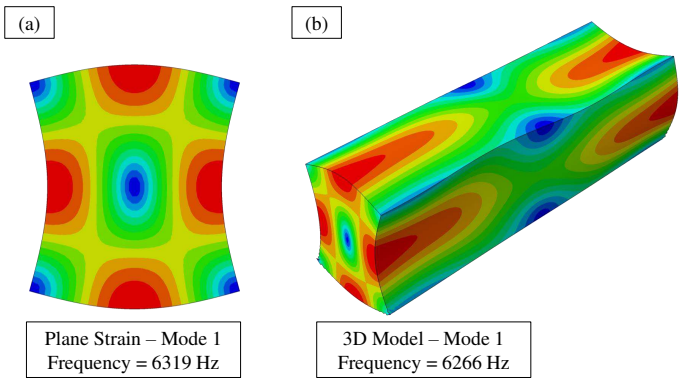

Fig. 1: Numerical simulations showing the fundamental IE mode of (a) the 2D (plane strain) model (f = 6319 Hz) and (b) the 3D model (f = 6266 Hz)

Figure 2(a) and (b) shows the second IE mode of the 2D (plane strain) and 3D models, with frequencies of 8830 Hz and 8845 Hz, respectively. The ratio between the frequencies of the second and the fundamental IE mode found in the 3D models is $f_2 = 1.41 f_1$, which agrees with the result given by Lin and Sansalone [15]. Furthermore, these frequencies agree with the measured frequencies on concrete specimens in this study. More details will be discussed in Section 5.1. The numerical simulation shows another resonance mode near the second IE mode, as seen in Figure 2(c). This mode is also found in our experiments, when the impact distance moved farther away from the receiver. The modes in Figs. 1(b) and 2(b) are symmetric in the longitudinal direction, while the mode in Fig. 2(c) involves a 180° rotation at one end of the beam.

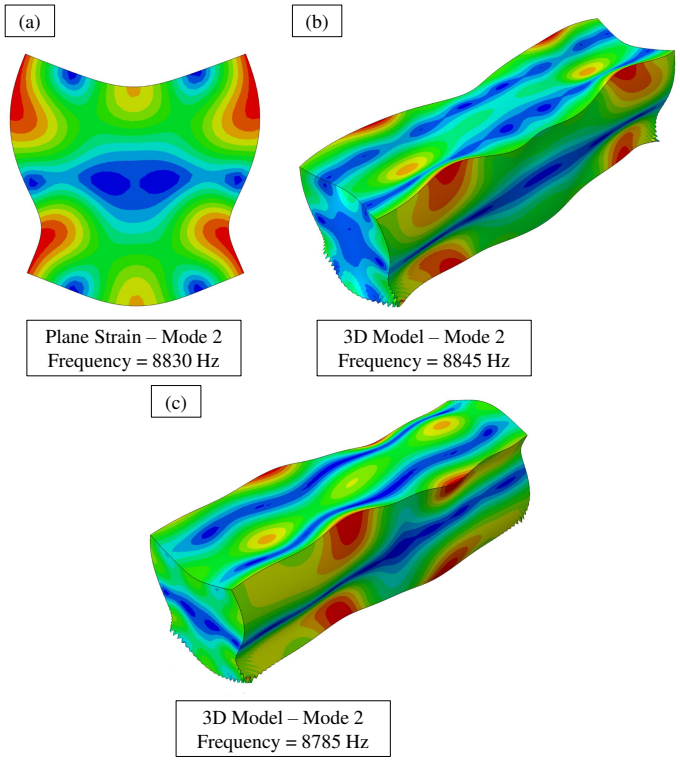

Fig. 2: Numerical simulations showing the second IE mode of (a) the 2D (plane strain) model ($f = 8830$ Hz), (b) the 3D model ($f = 8845$ Hz), and (c) an IE mode involving a 180° rotation at one end of the beam ($f = 8785$ Hz)

4 Concrete specimens and NDT experimental setup

4.1 Concrete specimens

In this project, seven specimens of various mix designs, lengths, and damage levels were tested to evaluate the versatility of the nonlinear IE test in quantitatively characterizing concrete damage. All specimens have a cross-section of 0.30 m × 0.30 m, as shown in Figure 3. In all confined specimens ("2D" specimens), #6 (diameter: 19 mm) headed reinforcement steel bars were used to constrain the expansion in the longitudinal and vertical directions.

Three different concrete mix designs (see Table 1) were utilized: (1) a control mix using innocuous local coarse and fine aggregates, (2) a reactive mix using a reactive coarse aggregate (RCA) and an innocuous local fine aggregate, and (3) a reactive mix using a reactive fine aggregate (RFA) and an innocuous local coarse aggregate. NaOH was added to the reactive mixes to boost the alkali content to 1.50% Na_2O_{eq} by mass of cement. One unconfined control specimen was tested, and each unconfined ASR damaged specimen has a 2D confined counterpart. Details of all seven specimens are summarized in Table 2.

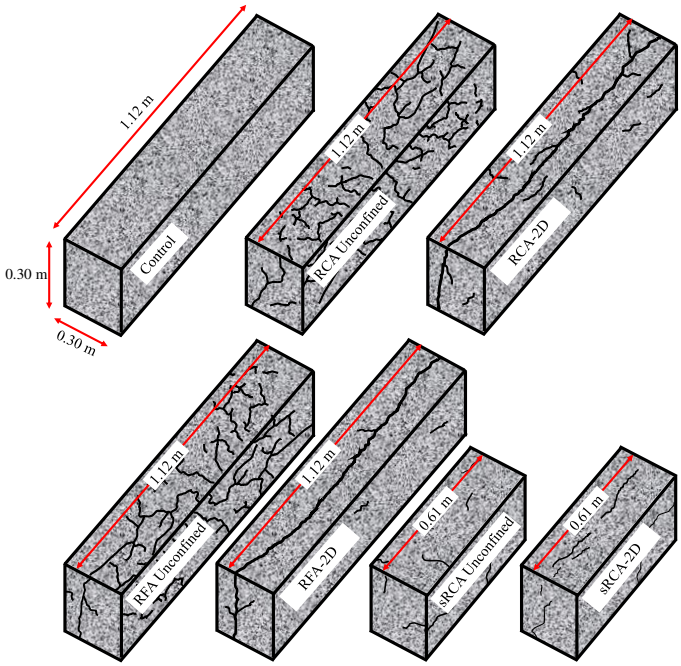

Fig. 3: Specimen design of Control, RCA Unconfined, RCA-2D, RFA Unconfined, RFA-2D, sRCA Unconfined, and sRCA-2D specimens

All specimens were moist cured for at least 28 days after casting. Then the specimens were moved to an environmental chamber for high temperature (38°C) and high humidity (95% RH) conditioning. The specimens were placed on carts to ensure all surfaces were exposed to moisture. An image of the seven test specimens in the

Table 1: Concrete Mix Design (SSD) and Strength

Component	Control (kg/m^3)	RCA (kg/m^3)	RFA (kg/m^3)
Cement	350	350	350
Water	175	175	175
Coarse aggregate	1127	1039	1095
Fine aggregate	709	839	743
Water reducer	2.3 mL/kg	2.3 mL/kg	2.3 mL/kg
50/50 NaOH	0	9.31	9.31
w/c	0.50	0.50	0.50
28-day strength	37.2 MPa	32.7 MPa	32.8 MPa

Table 2: Concrete Specimen Information

Specimen	Dimension (m)	Mix design	Conditioning start date
Control	0.30×0.30×1.12	Control	11/27/2018
RCA Unc., RCA-2D	0.30×0.30×1.12	RCA	11/27/2018
RFA Unc., RFA-2D	0.30×0.30×1.12	RFA	04/04/2019
sRCA Unc., sRCA-2D	0.30×0.30×0.61	RCA	08/09/2019

environmental chamber is shown in Figure 4. Demountable mechanical strain gauges (DEMEC) were used to measure specimen expansions in the vertical, transverse, and longitudinal directions. Stainless steel DEMEC targets were epoxied on all surfaces (except for the bottom) of each specimen and in two directions on each surface. Every two weeks, the chamber was shut down overnight and then maintained at 23°C and 50% RH for 24 hours. Expansion measurements and IE testing were performed during the shutdown period when the internal temperature of the concrete specimens reached a stable temperature 23°C. Expansion measurements were conducted using 150 mm and 500 mm DEMEC strain gauges (Mayes Instruments Limited, UK). Three expansion measurements were taken in each direction on the specimens and were averaged. After all measurements were completed, the chamber was restarted, and the temperature and humidity resumed conditioning at 38°C and 95% RH.

The measured expansion of each test specimen throughout the conditioning period is shown in Figure 5. For the unconfined specimens, the expansion in the vertical and transverse directions are averaged, whereas the 2D reinforced specimen's vertical and transverse directional expansions are displayed separately as the confinement caused

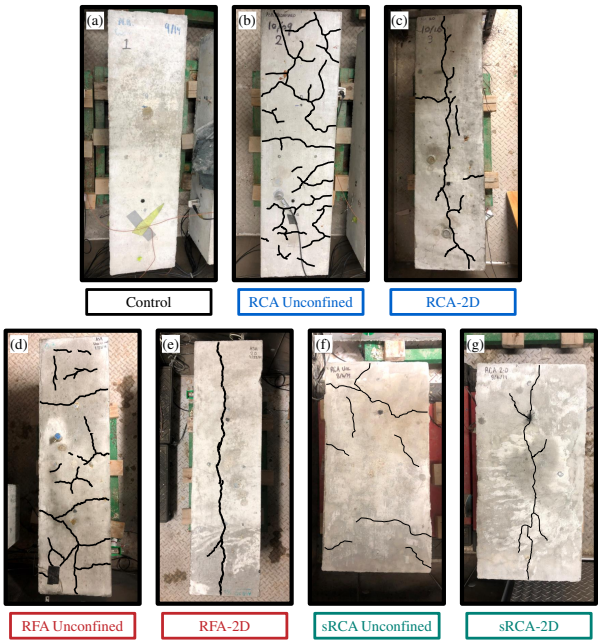

Fig. 4: Top surface of (a) Control, (b) RCA Unconfined, (c) RCA-2D, (d) RFA Unconfined, (e) RFA-2D, (f) sRCA Unconfined, and (g) sRCA-2D specimens. Images were taken at the end of the monitoring program.

different damage in each direction. IE testing began on the same date for all specimens, but because the specimens were cast at different times, the conditioning ages of specimens were different. The beginning of the IE testing period is indicated in Figure 5. Therefore, when the IE test began, the ASR specimens were in early, intermediate, and late stages of damage. By monitoring these specimens for more than 200 days, data was captured to evaluate the entire progression of ASR development.

4.2 Impact-echo mode determination

The impact response of the concrete specimens was measured using an accelerometer (PCB 352C65) with a sensitivity of 10.2 mV/(m/s^2). The accelerometer was connected to a signal conditioner (Brüel & Kjær 1704), and the analog signal was digitized by an oscilloscope (PICO 4262) with a sampling rate of 100 kS/s. The data acquisition

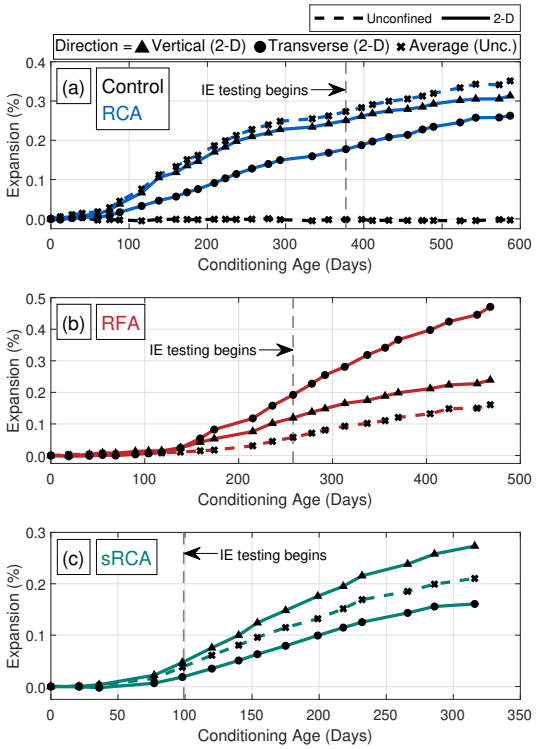

Fig. 5: Expansion measurement results during specimen conditioning for (a) Control, RCA Unconfined, RCA-2D, (b) RFA Unconfined, RFA-2D, (c) sRCA Unconfined, and sRCA-2D specimens in vertical and transverse directions for 2D confined specimens and the average of vertical and transverse directions for unconfined specimens

process was controlled by a LabVIEW program. Impacts were performed using a typical hammer with a mass of 200 g.

In a beam member, multiple IE modes and global vibration modes can be excited by an impact. It can sometimes be difficult to conclusively determine which mode is the fundamental IE mode, since multiple peaks (modes) exist in the frequency spectrum. Global modes are affected by the impact location, support conditions, and beam length. The IE mode is not affected by support conditions and is present at each impact location. Therefore, the IE mode can be determined by impacting the specimen at several locations and analyzing the signals collectively. This multi-impact technique

is proposed to conclusively determine the fundamental IE frequency. The experimental setup for IE mode determination is shown in Figure 6(a). The accelerometer was placed approximately 35 cm from the end of the 1.12 m specimen to avoid influence from the boundary. For the 0.61 m specimen, the accelerometer was placed 15 cm from the end of the specimen. The specimen was then impacted at a spacing of 5 cm.

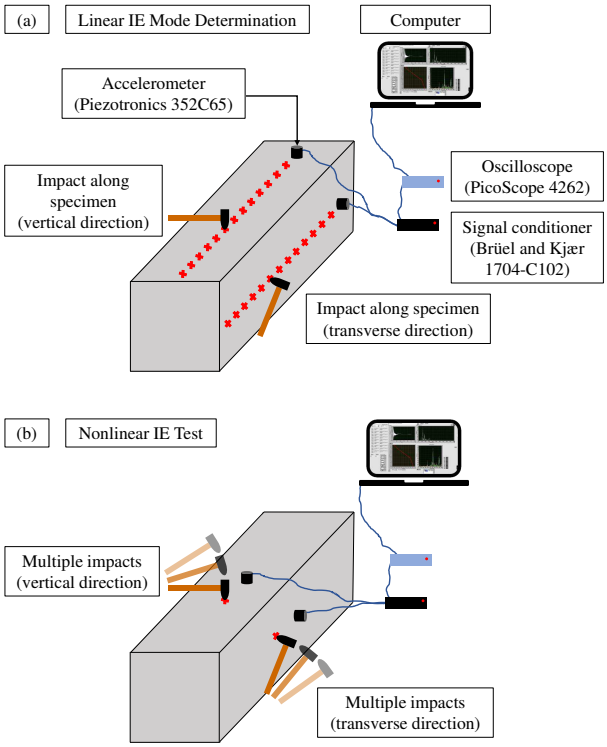

Fig. 6: Experimental setup for (a) linear impact-echo mode determination and (b) nonlinear impact-echo testing

4.3 Nonlinear impact-echo test setup

After the IE frequency was determined, the nonlinear IE test was conducted in two directions (vertical and transverse) on each specimen. The experimental setup for the nonlinear IE test is shown in Figure 6(b). The accelerometer was fixed at the

center position on the side of the beam being tested and was not moved throughout the test. Multiple impacts were conducted near the accelerometer with increasing impact amplitudes. The test procedure is similar to the NIRAS method. As the impact amplitude increases, the IE frequency decreases. The relationship between impact amplitude and IE frequency shift is used to determine the nonlinearity of the specimen. A LabVIEW program was designed to ensure that the amplitudes of the impacts used to generate the frequency spectra were as uniformly distributed as possible. For the 2D confined specimens, the nonlinear IE test was conducted on the top surface by impacting in the vertical direction and side surface by impacting in the transverse direction. Due to the confinement in the vertical and longitudinal directions, the ASR damage in each direction was distinct. For the unconfined specimens, it was found that the two directions showed similar nonlinear IE results because the ASR damage was uniform. Therefore, for the unconfined specimens, the nonlinear IE results in the vertical and transverse directions were averaged and taken as representative of the overall damage state of the specimen.

Figure 7(a) details the process of stacking multiple frequency domain signals across three specimen types (Control, sRCA Unconfined, and RCA Unconfined). For specimens at higher damage levels, a larger decrease in resonance frequency was observed with increasing amplitude. The nonlinear parameter (α) was then determined by plotting the resonance frequency shift $(f_0 - f)/f_0$ against the acceleration amplitude and calculating the respective slope of the relationship, as shown in Figure 7(b).

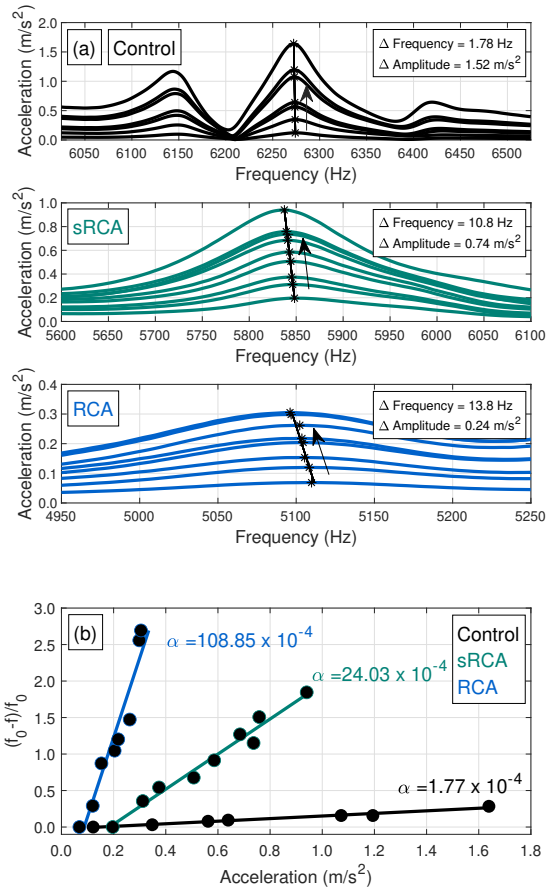

Fig. 7: Impact-echo signals and analysis including (a) frequency spectra and (b) multi-impact nonlinear analysis for the following specimens in the respective testing directions: Control vertical direction (vertical expansion of -0.007%), sRCA Unconfined transverse direction (transverse expansion of 0.057%), and RCA Unconfined transverse direction (transverse expansion of 0.209%) from tests performed on 01/08/2020

5 Results and discussions

5.1 Impact-echo mode determination

Figure 8(a) shows a typical frequency spectrum generated from an impact on the Control specimen in the vertical direction. A 2D frequency spectrum image was formed by stacking a series of frequency-domain signals with different impact locations along

the length of the beam presented in a color image (see Figure 8(b)). The frequency spectrum of the specific impact displayed in Figure 8(a) is marked with a dashed line in the 2D frequency spectrum image shown in Figure 8(b). The first vertical strip, which varied from 6221 Hz to 6269 Hz, represents the fundamental IE mode (found at an average frequency of $f_1 = 6256$ Hz). The second vertical strip represents the second IE mode (found at a frequency of approximately $f_2 = 8850$ Hz). Similar to the results of the numerical analysis (see Section 3), the ratio between the frequencies of the second and the fundamental IE mode is $f_2 = 1.41 f_1$, which aligns with the result given by Lin and Sansalone [15]. The numerical simulation predicts another mode that is very similar to the second IE mode but has a slightly lower frequency, which is also observed in the experiment. The second strip shifts to the left from 8848 Hz to 8776 Hz when the impact was applied at a large distance (> 75 cm). The third strip does not correspond to any mode in the numerical simulation. Therefore, it may be a global vibration mode for the specific beam length and support conditions.

Figure 9(a) shows a typical frequency spectrum generated from an impact on the sRCA Unconfined specimen in the vertical direction. The first vertical strip, which varied from 6071 Hz to 6104 Hz, represents the fundamental IE mode (found at an average frequency of $f_1 = 6084$ Hz). The second vertical strip represents the second IE mode (found at a frequency of approximately $f_2 = 8815$ Hz). The B-scan image shown in Figure 9(b), however, is less clear than that of the Control specimen (Figure 8(b)), which indicates the presence of damage and increased damping.

Figure 10(a) shows a typical frequency spectrum generated from an impact on the RFA-2D specimen in the vertical direction. Figure 10(b) shows the B-scan image of multiple impacts at different locations. The first vertical strip, which varied from 5500 Hz to 5586 Hz, represents the fundamental IE mode (found at an average frequency of $f_1 = 5555$ Hz). The second vertical strip represents the second IE mode (found at a frequency of approximately $f_2 = 7810$ Hz). The IE frequency is lower than that of

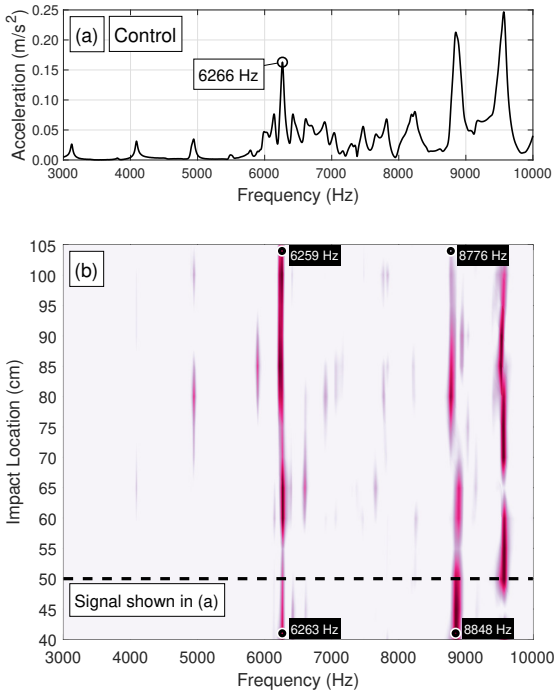

Fig. 8: IE results in the vertical direction of the Control specimen: (a) Frequency spectrum for a single impact at 50 cm, (b) B-scan image for multiple impact analysis (average fundamental IE mode $f_1 = 6256$ Hz)

the Control specimen, which indicates greater damage and low velocity. The fundamental and secondary frequency strip are quite blurry, indicating severe damage in the specimen.

For the specimens with a square cross-section in this study, the fundamental IE mode is easy to identify using the presented method. For more complex cases, time-frequency analysis and multichannel analysis of surface waves (MASW) method [20] can be used to build the dispersion curves to identify the cutoff modes and ZGV modes.

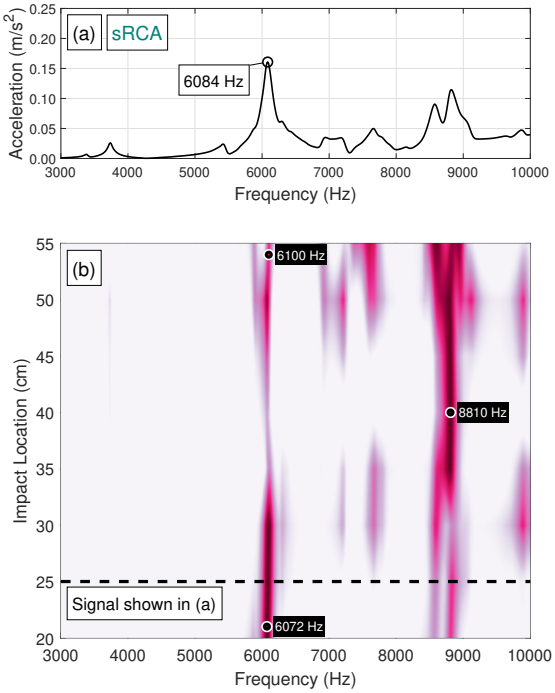

Fig. 9: IE results in the vertical direction of the sRCA Unconfined specimen (vertical expansion of 0.021%): (a) Frequency spectrum for a single impact at 25 cm, (b) B-scan image for multiple impact analysis (average fundamental IE mode $f_1 = 6084$ Hz)

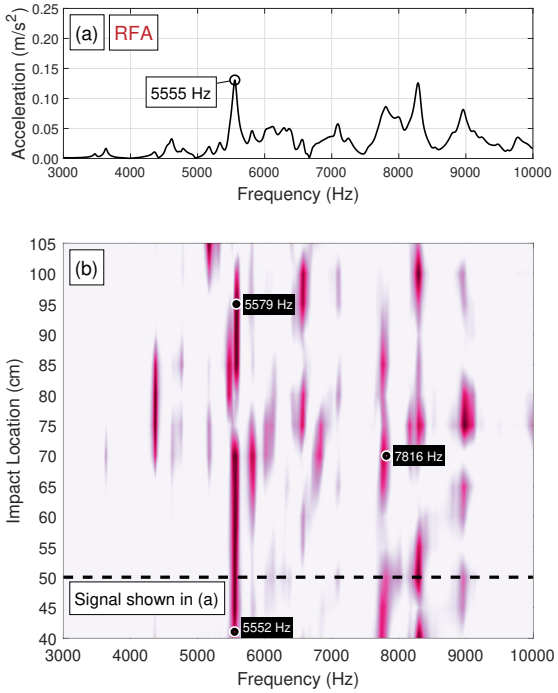

Fig. 10: IE results in the vertical direction of the RFA-2D specimen (vertical expansion of 0.068%): (a) Frequency spectrum for a single impact at 50 cm, (b) B-scan image for multiple impact analysis (average fundamental IE mode $f_1 = 5555$ Hz)

5.2 Linear impact-echo results

The fundamental IE mode frequency has been used in both linear and nonlinear analyses. A series of impacts with increasing amplitude were used in the nonlinear IE test, in which the peak IE frequency of the impact with the lowest impact amplitude was taken as the linear IE frequency of each specimen.

Figure 11 presents the progression of the linear IE frequency of all specimens with the conditioning age over the monitoring period. The average linear Control IE measurement ($f = 6255$ Hz) was taken as a representative baseline for all seven specimens, because the IE frequency of the Control specimen was stable throughout the entire monitoring period. The normalized linear IE frequency was taken as a percentage of the linear IE frequency of each specimen compared to the average Control linear IE frequency.

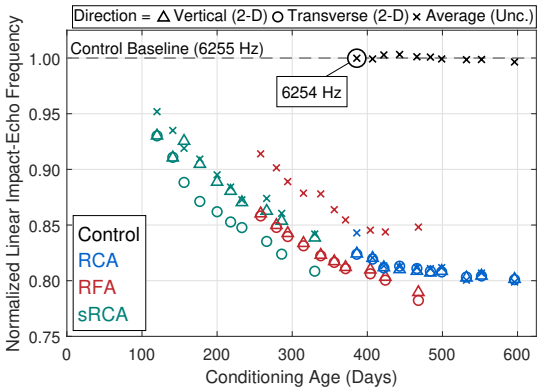

Fig. 11: Normalized linear IE frequency for all specimens. Frequencies in vertical and transverse directions are plotted for 2D confined specimens, and the average frequency in vertical and transverse directions are plotted for unconfined specimens

Although the specimens were cast at different date and have different confinement conditions, the data shows a clear decreasing trend with conditioning ages. Because the IE monitoring started after 100 days of conditioning on the sRCA specimens, the initial frequency drop date was not captured, which may indicate the initiation of

ASR expansion. By extrapolating the data to the earlier date, it is found that the frequency drop started around 80 days of conditioning. The IE frequency decreased fast in the first 300 days, and then became saturated at 80%, although specimen expansion was still progressing (as seen in Figure 5). The influence of cracking on the elastic modulus of the specimens reached a maximum, and the linear IE frequency was no longer sensitive to further damage development. This result is consistent with previous findings for resonance frequency testing on ASR damaged concrete prisms by Malone et al. [21], Rivard and Saint-Pierre [22], and Giannini et al. [23]. A study of monitoring the relative ultrasonic velocity change in the same group of specimens by Sun et al. [24] also indicated saturation at a velocity drop of 20%.

The IE frequency of a specimen is dependent on the depth and material properties (velocity, density, modulus, Poisson's ratio) of the specimen. Slight variations in specimen dimensions or materials will affect the IE frequency. The IE frequency progression of the six ASR specimens follow the same general trend, except for the RFA data. The RFA Unconfined specimen had IE frequencies shifted higher than the rest of the test specimens. Ideally, a baseline IE frequency measurement is available for each specimen. The baseline frequency data is not available in this study, so the IE frequency on the control specimens is used for normalization. If the RFA specimen had a higher initial frequency, normalization by the control specimen's frequency will shift the data higher. Therefore, it is not possible to directly compare the IE frequencies measured from different specimens and draw a conclusion about the health of the specimen. To be able to interpret the damage state of the specimen, a baseline measurement is needed.

5.3 Nonlinear impact-echo results

The nonlinear IE test was performed during the conditioning period to monitor specimen damage development. Microcracking present from ASR increased the material nonlinearity, due to clapping and friction at the crack interfaces under external excitement. Figure 12 plots progression of the normalized nonlinear parameter (α) with conditioning age for the Control, RCA Unconfined, RCA-2D, RFA Unconfined, RFA-2D, sRCA Unconfined, and sRCA-2D specimens. Results were normalized to the average nonlinear parameter (α) value found for the Control specimen ($\alpha = 2.40\times10^{-4}$). During the monitoring period it was observed that as conditioning time increased for the reactive specimens, damage increased, and the nonlinear parameter (α) determined by nonlinear IE testing increased. At the end of monitoring, the nonlinear parameter in all reactive specimens increased 50 to 100 times compared to the control specimen. The Control specimen did not show any damage, and the nonlinear parameter (α) had negligible change and remained around a value of 2×10^{-4} during the testing period. The results indicate that the nonlinear IE test is sensitive to detecting damage in concrete specimens, even at late ages. The measured nonlinear parameter (α) increased throughout the whole duration of the test and did not become saturated past a certain damage level, unlike the linear IE results.

The six ASR damaged specimens followed the same general rate of nonlinear parameter (α) increase during the testing period, except for the transverse direction of the RFA-2D specimen. The parameter in transverse direction of the RFA-2D specimen increased at a significantly faster rate than in other specimens. Looking at Figure 5, the transverse direction expansion of the RFA-2D specimen was the largest among the ASR damaged specimens. This expansion can be practically seen in Figure 4, where a large crack in the longitudinal direction is shown on the top surface of the RFA-2D specimen as a result of substantial transverse expansion. The increased damage in this

direction resulted in a higher measurement of nonlinear parameter (α) throughout the testing period.

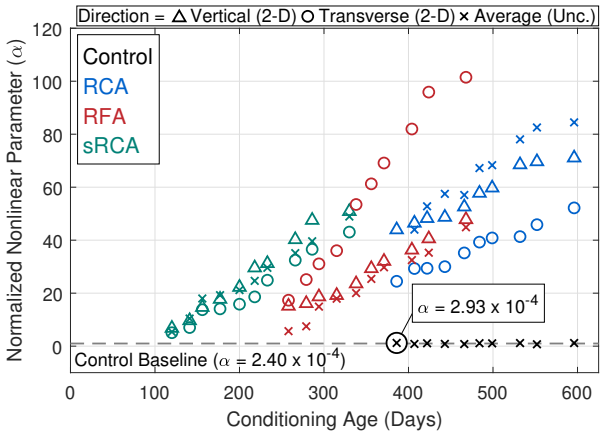

Fig. 12: Normalized nonlinear IE measurement results for all specimens in vertical and transverse directions for 2D confined specimens and the average of vertical and transverse directions for unconfined specimens

5.4 Quantitative correlation of nonlinear results and ASR expansion

Figure 13 compares the progression of the nonlinear parameter (α) of all specimens with their respective directional expansions at the time of nonlinear testing over the course of the testing period. The results across all specimens form a nearly linear relationship, regardless of their mix design, type of reactive aggregate, or specimen length. The strong linear correlation indicates that both the expansion and nonlinear response are governed by the same parameter related to ASR damage during the monitoring period, crack density. A similar finding was also observed on small concrete prisms using the NIRAS test [21], in which the prisms had the similar mix designs as the large specimens in this study.

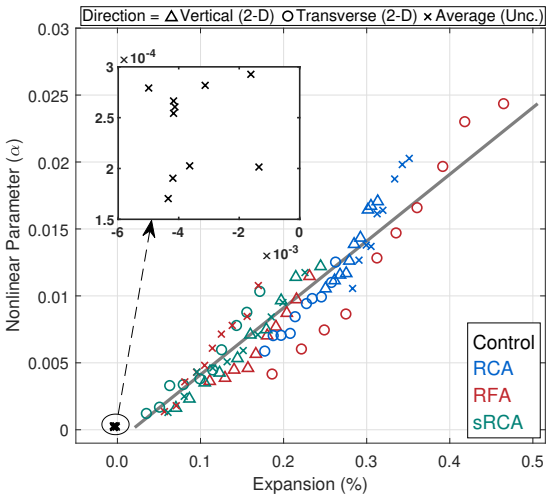

Fig. 13: Relationship between nonlinear parameter (α) and specimen expansion for the Control, RCA Unconfined, RCA-2D, RFA Unconfined, RFA-2D, sRCA Unconfined, and sRCA-2D specimens in vertical and transverse directions for 2D confined specimens and the average of vertical and transverse directions for unconfined specimens

The repeatability of this test is presented in the consistency of the measurements on the Control specimen over the entire testing period. A total of ten nonlinear IE tests were performed on each specimen over the testing period. As there was no damage development in the Control specimen, it was assumed that the nonlinearity of the specimen would remain relatively unchanged. Over the course of the testing period, the values of nonlinear parameter (α) on the six ASR damaged specimens ranged from 12.2×10^{-4} to 244×10^{-4}. However, the values of nonlinear parameter (α) on the Control specimen only ranged from 1.70×10^{-4} to 2.93×10^{-4}, with a mean value ($\bar{X}$) $= 2.40\times10^{-4}$ and standard deviation (σ) $= 0.42\times10^{-4}$. The low variance in the measurements on the Control specimen (displayed in Figure 13), taken over more than 200 days, instills confidence in the consistency and repeatability of the nonlinear IE test.

The relationship shown for the ASR specimens indicates the possibility that the nonlinear IE method can be used to quantitatively evaluate ASR damage by correlating the nonlinear parameter (α) to specimen expansion. Unlike an expansion measurement or the linear IE test, which needs a baseline (initial value), the nonlinear parameter (α) from the nonlinear IE test can be measured at any time without a reference measurement. The measured nonlinear parameter (α) is highly sensitive to specimen cracking but is not affected by other factors such as aggregate type or specimen length, and therefore can be used for quantitative evaluation of ASR damage.

6 Conclusions

This paper presents the nonlinear IE test for concrete ASR damage evaluation. By combining the practical advantages of the IE test with the high sensitivity of nonlinear acoustic analysis, the proposed nonlinear IE test method provides a practical solution for evaluation of large concrete specimens with improved accuracy. The nonlinear IE method was validated on concrete beam specimens of different lengths with different levels of ASR damage. Major findings from the experimental studies are shown below:

1. The nonlinear IE test method is easy to apply and the test results are not affected by the length and support condition of the specimens. Therefore, this method is applicable for damage evaluation on large specimens.
2. Many vibration modes are excited in a beam or column member by an impact. Therefore, it is sometimes challenging to identify the fundamental IE mode. In this study, multiple impacts were used at different locations and the frequency spectra were stacked to identify the IE modes.
3. Monitoring the fundamental linear IE frequency over the testing period allowed for evaluation of ASR damage in the concrete specimens. However, a baseline measurement is needed. In addition, the IE frequency drop became saturated at approximately 20% and stopped decreasing, although the ASR damage was still

progressing. Therefore, the linear analysis of IE test signals is useful only when a baseline measurement is available and when concrete damage is in early or medium stages.

4. The nonlinear IE method is highly sensitive to ASR damage and was used to detect damage in the six different ASR damaged specimens in this study. The largest nonlinear parameter (α) occurred in the RFA-2D specimen in the transverse direction, with a final value of 244×10^{-4} (at a transverse expansion of 0.465%). This value is about 100 times larger than the average value of the Control specimen. The nonlinear parameter (α) continued to increase proportionally to damage development and did not become saturated, while the linear frequency reached a maximum decrease and no longer could be used to monitor damage development. This phenomenon has been observed on other linear resonance tests and ultrasonic wave velocity monitoring on ASR specimens.
5. The test results display a nearly linear relationship between the nonlinear IE parameter (α) and ASR expansion that could be used to evaluate the damage level of a specimen without a baseline measurement. The relationship indicates the results obtained from the nonlinear IE test are related to concrete cracking damage and are not affected by aggregate type or specimen length. Although the nonlinear IE test presented in this study was performed on beam members with square cross-sections, the authors believe it can also be applied to plates and other members that show similar thickness resonance modes. Therefore, the presented nonlinear IE test method may have broad applications to concrete structure evaluation.

Acknowledgments. This research is supported by the U.S. Department of Energy – Nuclear Energy University Program (NEUP) under the contract DE-NE0008544.

Declarations

- Funding U.S. Department of Energy DE-NE0008544.

- Conflict of interest The corresponding author Jinying Zhu is an associate editor of Journal of Nondestructive Evaluation.
- Ethics approval Not applicable
- Consent to participate Not applicable
- Consent for publication The publisher has the author's permission to publish this paper and the research findings within it.
- Availability of data and materials The data that support the findings of this study are available from the corresponding author J.Z. upon reasonable request.
- Code availability The code is available upon reasonable request.
- Authors' contributions J.Z. and C.M. conceptualized the methodology. C.M. collected data and performed analysis. All authors wrote, edited, and reviewed the manuscript.

References

[1] Van Den Abeele KEA, Carmeliet J, Ten Cate JA, Johnson PA. Nonlinear elastic wave spectroscopy (NEWS) techniques to discern material damage, Part II: Single-mode nonlinear resonance acoustic spectroscopy. Journal of Research in Nondestructive Evaluation. 2000;12(1):31–42.

[2] Chen J, Jayapalan AR, Kim JY, Kurtis KE, Jacobs LJ. Rapid evaluation of alkali–silica reactivity of aggregates using a nonlinear resonance spectroscopy technique. Cement and Concrete Research. 2010;40(6):914–923.

[3] ASTM Standard C215. Standard Test Method for Fundamental Transverse, Longitudinal, and Torsional Resonant Frequencies of Concrete Specimens. West Conshohocken, PA; 2019.

[4] Renaud G, Callé S, Defontaine M. Remote dynamic acoustoelastic testing: Elastic and dissipative acoustic nonlinearities measured under hydrostatic tension and

compression. Applied Physics Letters. 2009;94(1):011905.

[5] Renaud G, Talmant M, Callé S, Defontaine M, Laugier P. Nonlinear elastodynamics in micro-inhomogeneous solids observed by head-wave based dynamic acoustoelastic testing. The Journal of the Acoustical Society of America. 2011;130(6):3583–3589.

[6] Shokouhi P, Rivière J, Lake CR, Le Bas PY, Ulrich T. Dynamic acousto-elastic testing of concrete with a coda-wave probe: comparison with standard linear and nonlinear ultrasonic techniques. Ultrasonics. 2017;81:59–65.

[7] Zhang Y, Larose E, Moreau L, d'Ozouville G. Three-dimensional in-situ imaging of cracks in concrete using diffuse ultrasound. Structural Health Monitoring. 2018 Mar;17(2):279–284. https://doi.org/10.1177/1475921717690938.

[8] Basu S, Thirumalaiselvi A, Sasmal S, Kundu T. Nonlinear ultrasonics-based technique for monitoring damage progression in reinforced concrete structures. Ultrasonics. 2021;115:106472. https://doi.org/10.1016/j.ultras.2021.106472.

[9] ASTM Standard C1383. Standard Test Method for Measuring the P-Wave Speed and the Thickness of Concrete Plates Using the Impact-Echo Method. West Conshohocken, PA; 2015.

[10] Gibson A, Popovics JS. Lamb wave basis for impact-echo method analysis. Journal of Engineering mechanics. 2005;131(4):438–443.

[11] Prada C, Clorennec D, Royer D. Local vibration of an elastic plate and zero-group velocity Lamb modes. The Journal of the Acoustical Society of America. 2008 Jul;124(1):203–212. https://doi.org/10.1121/1.2918543.

[12] Sansalone MJ, Streett WB. Impact-echo: Nondestructive Evaluation of Concrete and Masonry. Bullbrier Press; 1997.

[13] Laurent J, Royer D, Hussain T, Ahmad F, Prada C. Laser induced zero-group velocity resonances in transversely isotropic cylinder. The Journal of the Acoustical Society of America. 2015;137(6):3325–3334. https://doi.org/10.1121/1.4921608.

[14] Hayashi T, Song WJ, Rose JL. Guided wave dispersion curves for a bar with an arbitrary cross-section, a rod and rail example. Ultrasonics. 2003 May;41(3):175–183. https://doi.org/10.1016/S0041-624X(03)00097-0.

[15] Lin Y, Sansalone M. Transient response of thick circular and square bars subjected to transverse elastic impact. The Journal of the Acoustical Society of America. 1992 Feb;91(2):885–893.

[16] Guyer RA, McCall KR, Boitnott GN. Hysteresis, Discrete Memory, and Nonlinear Wave Propagation in Rock: A New Paradigm. Physical Review Letters. 1995;74(17):3491–3494.

[17] Van Den Abeele KEA, Johnson PA, Sutin A. Nonlinear elastic wave spectroscopy (NEWS) techniques to discern material damage, part I: nonlinear wave modulation spectroscopy (NWMS). Journal of Research in Nondestructive Evaluation. 2000;12(1):17–30.

[18] Jin J, Moreno MG, Riviere J, Shokouhi P. Impact-based nonlinear acoustic testing for characterizing distributed damage in concrete. Journal of Nondestructive Evaluation. 2017;36(3):51.

[19] Johnson PA, Zinszner B, Rasolofosaon PN. Resonance and elastic nonlinear phenomena in rock. Journal of Geophysical Research: Solid Earth.

1996;101(B5):11553–11564.

[20] Bjurström H, Ryden N. Detecting the thickness mode frequency in a concrete plate using backward wave propagation. The Journal of the Acoustical Society of America. 2016 Feb;139(2):649–657. https://doi.org/10.1121/1.4941250.

[21] Malone C, Zhu J, Hu J, Snyder A, Giannini E. Evaluation of alkali–silica reaction damage in concrete using linear and nonlinear resonance techniques. Construction and Building Materials. 2021;303:124538.

[22] Rivard P, Saint-Pierre F. Assessing alkali-silica reaction damage to concrete with non-destructive methods: From the lab to the field. Construction and Building Materials. 2009 Feb;23(2):902–909.

[23] Giannini ER, Folliard KJ, Zhu J, Bayrak O, Kreitman K, Webb Z, et al.: Non-destructive evaluation of in-service concrete structures affected by alkali-silica reaction (ASR) or delayed ettringite formation (DEF)– Final Report, Part I.

[24] Sun H, Tang Y, Malone C, Zhu J. Long-term ultrasonic monitoring of concrete affected by alkali-silica reaction. Structural Health Monitoring. 2023;22(4). https://doi.org/10.1177/14759217231169000.